Nonlinear optical absorption of few-layer molybdenum diselenide ($MoSe_2$) for passively mode-locked soliton fiber laser [Invited]

Zhengqian Luo,[1,*] Yingyue Li,[1] Min Zhong,[1] Yizhong Huang,[1] Xiaojiao Wan,[1] Jian Peng,[2] and Jian Weng[2,3]

[1]*Department of Electronic Engineering, Xiamen University, Xiamen 361005, China*
[2]*Department of Biomaterials, College of Materials, Xiamen University, Xiamen 361005, China*
[3]*e-mail: jweng@xmu.edu.cn*
**Corresponding author: zqluo@xmu.edu.cn*

Received January 6, 2015; revised March 12, 2015; accepted March 12, 2015;
posted March 13, 2015 (Doc. ID 231765); published April 20, 2015

In this paper, both nonlinear saturable absorption and two-photon absorption (TPA) of few-layer molybdenum diselenide ($MoSe_2$) were observed at 1.56 μm wavelength and further applied to mode-locked ultrafast fiber laser for the first time to our knowledge. Few-layer $MoSe_2$ nanosheets were prepared by liquid-phase exfoliation method and characterized by x ray diffractometer, Raman spectroscopy, and atomic force microscopy. The obtained few-layer $MoSe_2$ dispersion is further composited with a polymer material for convenient fabrication of $MoSe_2$ thin films. Then, we investigated the nonlinear optical (NLO) absorption property of the few-layer $MoSe_2$ film using a balanced twin-detector measurement technique. Both the saturable absorption and TPA effects of the few-layer $MoSe_2$ film were found by increasing the input optical intensity. The saturable absorption shows a modulation depth of 0.63% and a low nonsaturable loss of ~3.5%, corresponding to the relative modulation depth of 18%. The TPA effect occurred when the input optical intensity exceeds ~260 MW/cm^2. Furthermore, we experimentally exploit the saturable absorption of few-layer $MoSe_2$ film to mode lock an all-fiber erbium-doped fiber laser. Stable soliton mode locking at 1558 nm center wavelength is achieved with pulse duration of 1.45 ps. It was also observed that the TPA process suppresses the mode-locking operation in the case of higher optical intensity. Our results indicate that layered $MoSe_2$, as another two-dimensional nanomaterial, can provide excellent NLO properties (e.g., saturable absorption and TPA) for potential applications in ultrashort pulse generation and optical limiting.

OCIS codes: (160.4236) Nanomaterials; (160.4330) Nonlinear optical materials; (060.3510) Lasers, fiber; (140.4050) Mode-locked lasers.
http://dx.doi.org/10.1364/PRJ.3.000A79

1. INTRODUCTION

Nonlinear optical (NLO) responses can play an important role in light–matter interaction, and have attracted intense interest for use in versatile photonic and optoelectronic applications [1]. Optical materials under high-intensity laser field can show some fantastic NLO effects, including nonlinear absorption [2], Kerr nonlinearity, and Raman/Brillouin scattering [3,4]. Among them, nonlinear absorption effect (e.g., saturable [5–10] and multiphoton [11,12] absorption) is always one of most important and intensive research topics. For example, saturable absorption is usually used to generate short laser pulses by passive mode-locking [13–20] or *Q*-switching [21–24] techniques. Multiphoton absorption can be very useful for applications in optical limiting [25] and fluorescence microscopy [26]. Generally, these NLO responses are extremely dependent on the optical materials themselves. Therefore, there is always great interest in developing new NLO materials.

Recently, it was found that two-dimensional (2D) materials (e.g., graphene [7,11]) can possess extraordinary NLO properties. Graphene, as the first-discovered 2D nanomaterial, has impressively exhibited strong NLO responses with a large nonlinear refractive index ($n_2 \sim 2 \times 10^{-7}$ cm$^2 \cdot$ W^{-1} [27]) and low saturable optical intensity of ~0.7 MW/cm^2 [7]. The nonlinear saturable absorption of graphene has been widely used to mode-lock/*Q*-switch lasers for short-pulse generation [28–36], and the Kerr nonlinearity (e.g., four-wave mixing) of graphene has also been applied to wavelength conversion [37].

The success of graphene has triggered a worldwide upsurge in research interest in 2D nanomaterials. In recent years, some new 2D materials [e.g., topological insulators (TIs)] have been successively discovered [38–47]. In particular, atomically thin group VIB transition metal dichalcogenides (TMDs; MX_2; M = W, Mo; X = S, Se), as a new class of 2D materials, have recently stimulated a great deal of research due to their unique and exotic properties. TMDs possess bandgap tunability by reducing the layer number or introducing the defects [48], high carrier mobility, and strong spin-orbit coupling, making them appealing materials for various applications in electronics and optics. Recent experiments have demonstrated that layered molybdenum diselenide ($MoSe_2$) has broadband saturable absorption from 400 to ~2100 nm [10,48], and exhibits a nonlinear refractive index ($n_2 \sim 0.2 \times 10^{-12}$ cm$^2 \cdot$ W^{-1}) [49]. Furthermore, mode-locking and *Q*-switching operations based on layered MoS_2 have been achieved at around 1, 1.5, and 2 μm [50–55]. However, it should be noted that most studies on the TMDs were focused on MoS_2 until now, and other TMDs (e.g., $MoSe_2$) have not yet been fully investigated.

Thin-layered $MoSe_2$ actually possesses more attractive properties compared with MoS_2, including narrower bandgap between 1.1 eV (indirect) and 1.5 eV (direct) [56], lower optical absorption coefficient [49], and larger spin-splitting energy of ~180 meV at the top of the valence bands. The narrow bandgap and low optical absorption coefficient could make $MoSe_2$ more applicable than MoS_2 to broadband saturable absorption for passively mode-locked lasers.

In this paper, we experimentally investigated the NLO absorption of few-layer $MoSe_2$ at 1.56 μm wavelength and further demonstrated a $MoSe_2$ passively mode-locked Er-doped fiber (EDF) soliton laser. Few-layer $MoSe_2$ was fabricated by the liquid-phase exfoliation (LPE) method and then embedded in polymer composite, constructing few-layer $MoSe_2$ films. Using a balanced twin-detector measurement system, the $MoSe_2$ film exhibited saturable absorption with a relative modulation depth of 18% and two-photon absorption (TPA) under the input optical intensity of >260 MW/cm^2. Furthermore, a mode-locked Er-doped fiber laser (ML-EDFL) based on a few-layer $MoSe_2$ film as saturable absorber (SA) was successfully achieved. The mode-locking operation could stably generate transform-limited pulses with a 1.45 ps duration, and was also interrupted by TPA under higher pumping level.

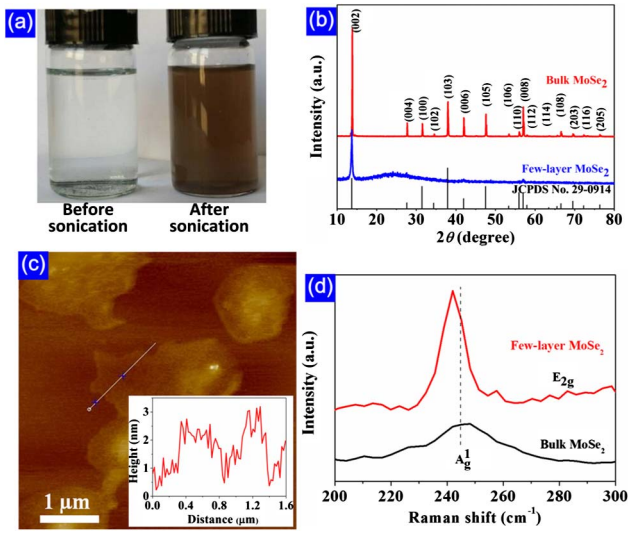

Fig. 1. Characterization of few-layer $MoSe_2$ by the LPE method. (a) $MoSe_2$ solution before (left) and after (right) sonication. (b) XRD patterns of the bulk $MoSe_2$ (top) and exfoliated few-layer $MoSe_2$ (bottom). (c) Typical AFM image and the height profile diagram (inset) of the few-layer $MoSe_2$ nanosheets. (d) Raman spectrum of the exfoliated $MoSe_2$.

2. PREPARATION AND CHARACTERIZATION OF $MoSe_2$

A. Few-Layer $MoSe_2$ Fabricated by the LPE Method

The few-layer $MoSe_2$ used in our experiment was prepared by the LPE method [57]. The LPE process for obtaining thin-layered 2D materials has two steps. Namely, bulk material is first mixed with a solvent and then sonicated under strong ultrasound field for overcoming the interlayer van der Waals forces. In this process, it is very key that a suitable solvent is chosen for easily exfoliating bulk crystals and stabilizing thin-layered material. It is required that the solvent surface energy be similar to the exfoliated material (e.g., $MoSe_2$). N-methyl-pyrrolidone, chitosan acetic, and Li^+ solutions were widely used to exfoliate graphene, TIs, and MoS_2 [38,44,50,55], but these solvents could be harmful to human health. In contrast, lysine is indispensable to human body and its surface energy is close to $MoSe_2$. Therefore, we used lysine as the dispersant to exfoliate and stabilize $MoSe_2$ in our experiment. Initially, the bulk $MoSe_2$ (325 mesh power, Alfa Aesar) was added into the 1 mg/mL lysine solution and sonicated for 20 h to produce the few-layer $MoSe_2$ suspension. The exfoliated $MoSe_2$ suspension was centrifuged for 30 min at 1000 rpm to remove bulk $MoSe_2$. Subsequently, the supernatant was decanted to another centrifuge tube. After centrifuging the supernatant at 13,000 rpm for 30 min to remove free lysine, the as-obtained product was collected into vials.

B. Characterization of Few-Layer $MoSe_2$

After exfoliation, the color of solution was deepened, manifesting that the exfoliated $MoSe_2$ had been well dispersed in lysine solution [Fig. 1(a)]. The purchased bulk $MoSe_2$ was first characterized by x ray diffraction (XRD). As shown in Fig. 1(b), all labeled peaks of the bulk material can be readily indexed to rhombohedral $MoSe_2$ (JCPDS no. 29-0914). Then, we measured the XRD pattern of the exfoliated $MoSe_2$. As given in Fig. 1(b), the high [002] orientation still exists and some characteristic peaks disappeared (compared to bulk structure), indicating that bulk $MoSe_2$ had been successfully exfoliated as we expected. The thickness of the as-prepared few-layer $MoSe_2$ was also characterized by atomic force microscopy (AFM), as shown in Fig. 1(c). The average thickness from the height profile diagram [inset of Fig. 1(c)] was measured to be ~2–3 nm. This indicates that the exfoliated $MoSe_2$ nanosheets are around 2–3 layers, because the single-layer thickness of $MoSe_2$ is about 0.8 nm [56]. In addition, it is well known that the location of Raman modes can also determine the thickness of 2D materials. Therefore, we further measured the Raman spectra [Fig. 1(d)] of $MoSe_2$ before and after exfoliation. We observed the prominent A_g^1 Raman mode, which is associated with the out-of-plane vibration of Se atoms. As shown in Fig. 1(d), the A_g^1 Raman mode of the as-exfoliated $MoSe_2$ is redshifted slightly, also confirming the few-layered structure of the as-prepared $MoSe_2$ [58]. Actually, the redshift phenomenon has been reported in other 2D materials (e.g., graphene, TIs, MoS_2), possibly originating from the decreasing the van der Waals forces between layers.

3. NLO ABSORPTION OF FEW-LAYER $MoSe_2$

To flexibly use the as-prepared $MoSe_2$ for practical applications, the polyvinyl alcohol (PVA) polymer was further dispersed into the few-layer $MoSe_2$ solution. Therefore, the $MoSe_2$ PVA film can be easily formed and transferred onto a fiber end-facet for constructing a fiber-compatible $MoSe_2$ device (see the $MoSe_2$ sample in Fig. 2).

Then, we measured the NLO absorption of the fiber-compatible $MoSe_2$ device using the balanced twin-detector measurement system (Fig. 2). The system consists of a femtosecond seed laser, erbium-doped fiber amplifier (EDFA), tunable optical attenuator, 50:50 coupler, and two optical powermeters. The seed laser from a homemade passively mode-locked fiber laser has a center wavelength of 1566 nm, pulse duration of ~650 fs, repetition rate of 22.15 MHz, and

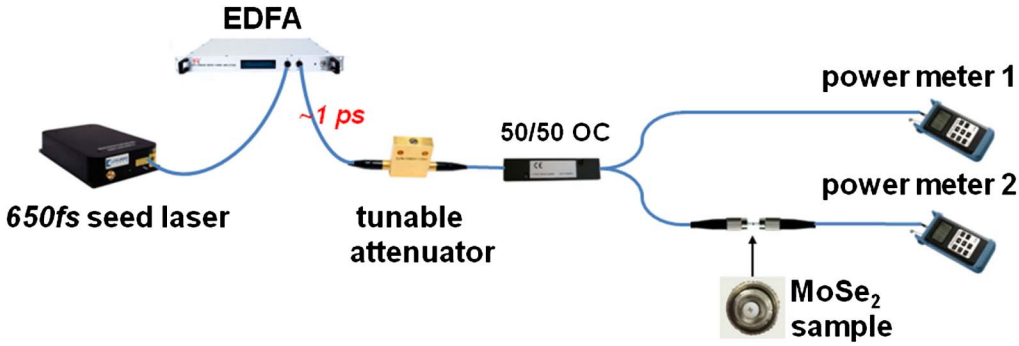

Fig. 2. Balanced twin-detector measurement system for measuring the NLO absorption of the fiber-compatible PVA-$MoSe_2$ film.

average output power of ~400 μW. When amplified by the EDFA, the optical power could reach ~10 mW, and the pulse duration was slightly broadened to ~1 ps. The amplified power was further divided by the 50:50 coupler and the 50% optical power could be injected into the few-layer $MoSe_2$ film (the other 50% being the reference beam). The tunable attenuator was used to continuously change the input optical intensity (I) into the $MoSe_2$ film. The maximum optical intensity into the $MoSe_2$ film can be ~500 MW/cm^2. As we increased the input optical intensity from 0.3 to 500 MW/cm^2, we recorded the optical absorbance of the few-layer $MoSe_2$ film. As shown in Fig. 3, the optical absorbance gradually reduces from 4.20% to 3.57% in the initial stage, but sharply increases when the input optical intensity is more than 260 MW/cm^2. The experimental data at the input optical intensity $I < 260$ MW/cm^2 can be well fitted by the formula

$$\alpha = \Delta\alpha/(1 + I/I_{\text{sat}}) + \alpha_{\text{linear}}. \quad (1)$$

Here, $\Delta\alpha$, I_{sat}, and α_{linear} represent the modulation depth, saturated optical intensity, and the nonsaturable loss, respectively. This clearly indicates that the saturable absorption behavior happens at $I < 260$ MW/cm^2, and has $\Delta\alpha = 0.63\%$, $I_{\text{sat}} = 19.8$ MW/cm^2, and a low nonsaturable loss $\alpha_{\text{linear}} = 3.57\%$. The normalized modulation depth can be calculated to be ~18%, comparable to that of graphene [7], TIs [41], and MoS_2 [52]. It is well known that, from the bulk to single-layer $MoSe_2$, the energy gap of $MoSe_2$ is between 1.1 eV (1.12 μm) and 1.5 eV (0.82 μm). It is noted that the 1.56 μm photon energy is less than the bandgap of $MoSe_2$, and one could question why the few-layer $MoSe_2$ has saturable absorption at the longer 1.56 μm wavelength. Similar to the few-layer MoS_2 reported previously [48–55], the saturable absorption of few-layer $MoSe_2$ at 1.56 μm can be well understood as being due to the following possible reasons: (1) the defects induced by the LPE fabrication process [48], and (2) the edge-state or surface absorption [55] (i.e., the coexistence of both semiconducting and metallic phases) [51–54].

Interestingly, we found that the experimental data at $I > 260$ MW/cm^2 can be well fitted by the quadratic equation as follows:

$$\alpha = \beta I^2 + \alpha_{\text{linear}}. \quad (2)$$

This shows that the TPA process in the few-layer $MoSe_2$ has been excited under the higher optical intensity, and the TPA coefficient β is 3.4×10^{-6} cm^4/MW^2. Note that the increasing of optical absorbance can be attributed to the TPA rather than the thermal damage of the $MoSe_2$ samples. This can be confirmed by the $MoSe_2$-based mode-locking operation features, and the reason will be further analyzed.

4. $MoSe_2$ PASSIVELY MODE-LOCKED FIBER SOLITON LASER

In this section, we will try to further exploit the NLO absorption effects (Fig. 3) of the few-layer $MoSe_2$ for laser application. The saturable absorption characteristic of few-layer $MoSe_2$ will especially be used for a passively mode-locked fiber laser.

A. Experimental Setup

Figure 4 shows the experimental setup of the EDFL passively mode-locked by the few-layer $MoSe_2$ film. A 974 nm laser diode (LD) is used to pump a section of 4.6 m EDF (Nufern,

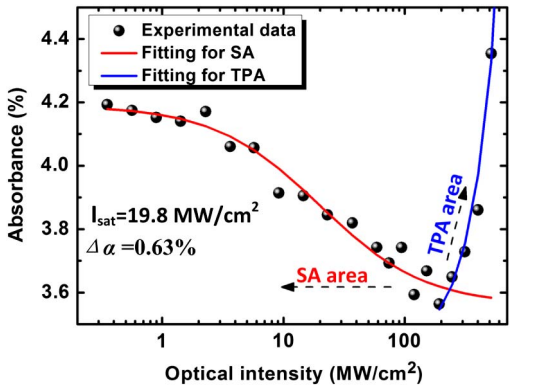

Fig. 3. Measured nonlinear absorption characteristics of the few-layer $MoSe_2$ film at 1566 nm wavelength. SA, saturable absorption.

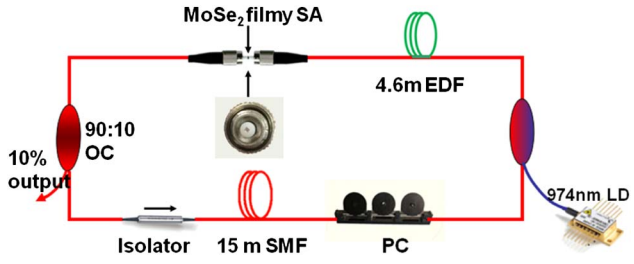

Fig. 4. Experiment setup of the proposed EDFL passively mode-locked by the few-layer $MoSe_2$ film.

EDFC-980-HP) through a 975/1550 nm wavelength division multiplexer. The EDF has an absorption coefficient of 3 dB/m at 980 nm and group velocity dispersion (GVD) of 53.6×10^{-3} ps^2/m at 1550 nm. The as-fabricated few-layer $MoSe_2$ device in the cavity acts as SA for passive mode locking. A polarization-independent isolator ensures the unidirectional laser operation. A polarization controller (PC) is used to fine tune the cavity birefringence for optimizing the mode-locking operation. A 10/90 optical coupler extracts 10% intracavity signal as laser output. In addition, a section of 15 m single-mode fiber with GVD of -22×10^{-3} ps^2/m at 1550 nm is used for ensuring the cavity operating in the anomalous dispersion region. The total cavity length is about 26 m, with net cavity dispersion of –0.224 ps^2. For measuring the laser outputs, the laser optical spectrum was monitored by an optical spectrum analyzer (HP 70951B), and a 10 GHz InGaAs photodetector (Nortel PP-10G-FAC) together with a 1 GHz digital oscilloscope used to detect the pulse trains and pulse waveforms. Moreover, the radio frequency (RF) output characteristics of the laser pulses were observed by a RF spectrum analyzer (Gwinstek GSP-930, 9 kHz–3 GHz), and the pulse duration was measured by an autocorrelator (FR-103XL, Femtochrome Research Inc.).

B. Experimental Results and Discussions

Because the net GVD of the cavity is anomalous, it can be expected that the ML-EDFL emits soliton pulses by the interplay between anomalous cavity dispersion and the fiber nonlinear Kerr effect. In our experiment, the laser oscillation started initially at continuous-wave (CW) regime at a low pump threshold of 5.5 mW. Then, the CW operation transited to a pulsed regime when the pump power exceeded 10.0 mW. Moreover, as we gradually increased the pump power from 10 to 30.2 mW, we found that the pulse repetition rate enlarged and pulse duration decreased, exhibiting the typical features of passive Q switching [21]. Actually, such passive Q switching under the lower pump power was observed usually in some passively mode-locked fiber lasers previously reported [18], mainly resulting from the few number of oscillating longitudinal modes and the insufficient nonlinearity in low pumping intensity. At the pump power of 17.4 mW, Fig. 5 gives the typical characteristics of the passive Q switching. The Q-switched optical spectrum [Fig. 5(a)] has a center wavelength of 1558.25 nm and a narrow 3 dB bandwidth of 0.28 nm. The typical oscilloscope trace [Fig. 5(b)] shows that the Q-switched pulse trains with an uniform pulse intensity have a periodic interval of 101 μs (corresponding to the repetition rate of 9.9 kHz). The inset of Fig. 5(b) further gives the single pulse envelope. The Gaussian-profile pulse has a pulse duration as broad as ~13.6 μs. The low repetition rate (kHz) and the relative broad pulses also suggest the occurrence of passive Q switching.

We interestingly found that, once the pump power is more than 30.3 mW, the passive Q-switching operation became unstable and could abruptly evolve into the mode-locking regime. Stable self-started mode-locking could be readily achieved by slightly adjusting the PC in the cavity. At the pump power of 33.4 mW, we measured the typical optical spectrum of this mode locking with a spectral resolution of 0.08 nm. As shown in Fig. 6(a), the mode-locked optical spectrum (solid line) was obviously broadened, compared with the

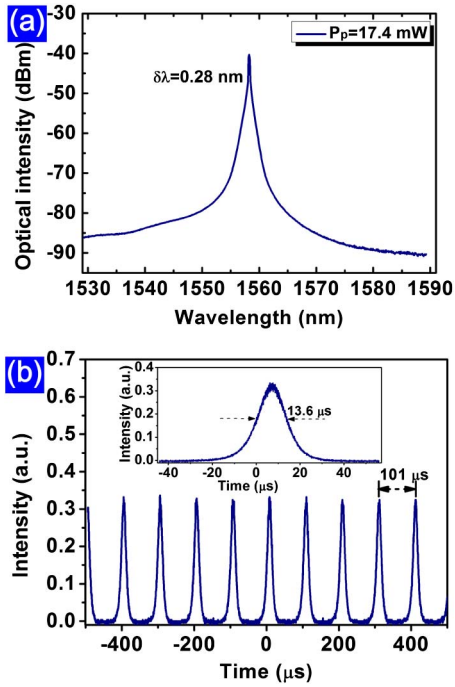

Fig. 5. (a) Optical spectrum and (b) typical oscilloscope trace of the passive Q-switching operation at the pump power of 17.4 mW. Inset, single-pulse envelope.

passive Q-switching one (dashed line). This implies that the mode-locking operation excited more longitudinal modes and also induced stronger optical nonlinearity in the laser. The mode-locking operation has a center wavelength of 1558.25 nm and a wide 3 dB bandwidth of 1.76 nm. Meanwhile, we clearly observed the symmetrical Kelly sidebands originating from the spectral interference of dispersive waves, manifesting that this operation was at the conventional solitary mode locking [59]. Moreover, the absence of additional narrow spectral peak also suggests that the soliton mode locking almost has no CW component. As shown in Fig. 6(b), we also measured the mode-locked pulse trains at the same pump power of 33.4 mW. The pulse interval of 124.5 ns matches well with the cavity roundtrip time (i.e., the cavity length of ~26 m), suggesting that only one soliton was generated per roundtrip. Furthermore, once the stable mode locking was obtained under the initial adjustment of the PC, we found in our experiment that the single soliton operation was always observed so long as the passive mode-locking state is not interrupted.

As shown in Fig. 7, the mode-locking operation at the pump power of 33.4 mW was further characterized by the RF spectrum analyzer and the autocorrelator. Figure 7(a) gives the output RF spectrum of the mode-locked pulses at the fundamental frequency peak for a scanning range of 50 kHz and RF resolution bandwidth of 10 Hz. The fundamental RF peak locates at 8.028 MHz, corresponding to the fundamental cavity repetition rate. This further confirms the occurrence of the passive mode locking. The RF signal-to-noise ratio (SNR) is more than 61.5 dB. We also measured the broadband RF spectrum with a large frequency span of 600 MHz. As can be seen in Fig. 7(b), the measured RF peaks from the 2nd- to 74th-order harmonic exhibit almost uniform intensity without spectral modulation. Both the higher RF SNR (>60 dB) and

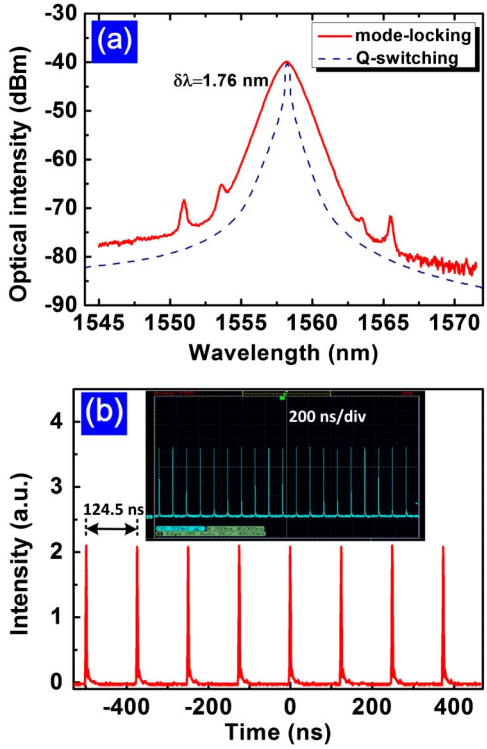

Fig. 6. (a) Mode-locked optical spectrum and (b) mode-locked pulse trains at the pump power of 33.4 mW.

the absence of modulation in the 600 MHz broad RF spectrum evidently indicate the good stability and CW mode-locking state of the proposed ML-EDFL. Figure 7(c) shows the measured autocorrelation trace of the mode-locked pulses with a narrow scanning range of 32 ps and time resolution of 100 fs. The full width at half maximum (FWHM) of the pulse was measured to be 2.23 ps. If the fit of sech^2 pulse shape is assumed, the corresponding pulse duration (τ) is 1.45 ps. The time–bandwidth product (TBP) of the mode-locked pulses can be further calculated by the equation

$$\mathrm{TBP} = \tau \times c \cdot \Delta\lambda/\lambda_0^2, \tag{3}$$

where c, λ_0, and $\Delta\lambda$ represent the light speed, center wavelength, and 3 dB bandwidth of the mode-locked optical spectrum. In our experiment, these parameters are $\tau = 1.45$ ps, $\lambda_0 = 1558.25$ nm, and $\Delta\lambda = 1.76$ nm, respectively. Therefore, the TBP of the mode-locked pulses is ~0.316. This manifests that the soliton mode locking of the proposed ML-EDFL generated the transform-limited pulses. Furthermore, an autocorrelation trace with a broad scanning range of 800 ps is given in Fig. 7(d). Note that no pedestal was shown on the autocorrelation trace [Fig. 7(d)], which reveals the excellent quality of the mode locking.

As we increased the pump power from 0 to 75 mW, we also recorded the average output power of the laser. One can see from Fig. 8(a) that the laser operation underwent four phases as follows: (1) the CW regime (pump power <10 mW); (2) the passive Q-switching regime (pump power in the range of 10 – 30.2 mW); (3) the soliton mode-locking regime (pump power from 30.3 to 73.5 mW); and (4) the CW regime (pump power >73.5 mW). The maximum average output power for passive mode locking is 440 μW, corresponding to the maximum pulse energy of 54.8 pJ. The obtained pulse energy is close to the theoretical calculation value of limited pulse energy (E_p) for a single soliton based on the formula [60]

$$E_p \approx 3.11\lambda_0^2/2\pi c\gamma|D_{\mathrm{av}}|/\tau. \tag{4}$$

Here, γ and $|D_{\mathrm{av}}|$ represent the nonlinear coefficient and the average dispersion of the laser cavity. In addition, one could

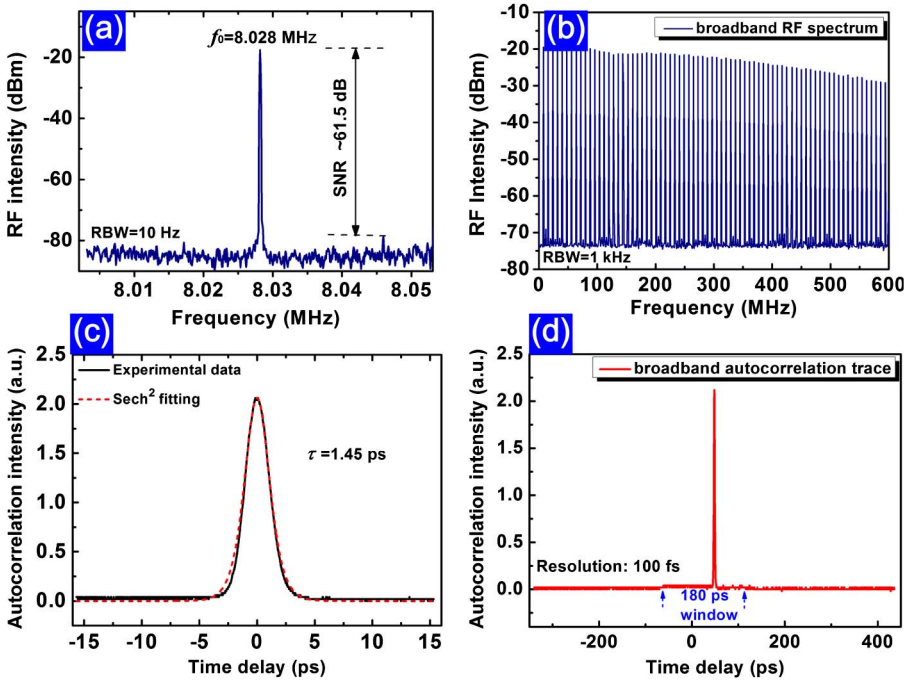

Fig. 7. (a) RF spectrum of the mode-locked pulses at the fundamental RF peak. (b) Broadband RF spectrum with a frequency span of 600 MHz. The autocorrelation traces of the mode-locked pulses with the (c) narrow and (d) broad scanning range are also shown.

question why the soliton mode locking degenerated in the case of pump power >50 mW (i.e., output average power >400 μW), and was even extinguished with pump power >73.5 mW. This phenomenon should be attributed to the TPA process of the few-layer $MoSe_2$ under intracavity high peak intensity. As shown in Fig. 3, when the optical intensity injected into the few-layer $MoSe_2$ film exceeds ~260 MW/cm^2, the SA performance becomes worse and the TPA process happens. In our experiment, when the output average power exceeds 400 μW, the intracavity power injected into the few-layer $MoSe_2$ film is more than 4 mW with 1.45 ps pulse duration, corresponding to the input optical intensity of ~300 MW/cm^2. Therefore, once the pump power is above 50 mW, TPA of the few-layer $MoSe_2$ film happens and the SA-based passive mode locking becomes worse. Decreasing the pump power from 75 mW to 0, we found in our experiment that the ML-EDFL exhibited optical bistability. Namely, when turning on or off the pump power, the processes of the laser operation are very different, as shown in Figs. 8(a) and 8(b). Laser operation with the decrease of pump power only underwent two phases, i.e., the soliton mode-locking (pump power from 73.5 to 8.5 mW) and CW regime (pump power <8.5 mW). Optical bistability has usually been observed in passively mode-locked fiber lasers based on other SAs (e.g., graphene [61] or TIs [41]), or the nonlinear amplifying loop mirror [62] or nonlinear polarization rotation techniques [63,64]. Komarov *et al.* [65,66] have numerically demonstrated that the optical bistability between the CW and mode-locked regimes is a common feature in fiber lasers independently of the exact optical configuration. Moreover, they also claimed that the mode locking would occur when the nonlinear transmission of the SA works as a positive feedback. The positive feedback means that the greater intensity produces the lower losses. In our experiment, when the fiber laser operated under the CW condition, the intracavity power intensity was much lower than that of mode-locking operation with the same pump power. Namely, the nonlinear loss caused by the SA is relatively larger than that of mode-locking operation. In order to initiate the mode locking from CW based on the saturable absorption of SAs, higher pump power is needed. Then the bistability can be observed in the fiber laser, which is in accordance with the numerical analyses [65,66] and experimental results [41,61–64].

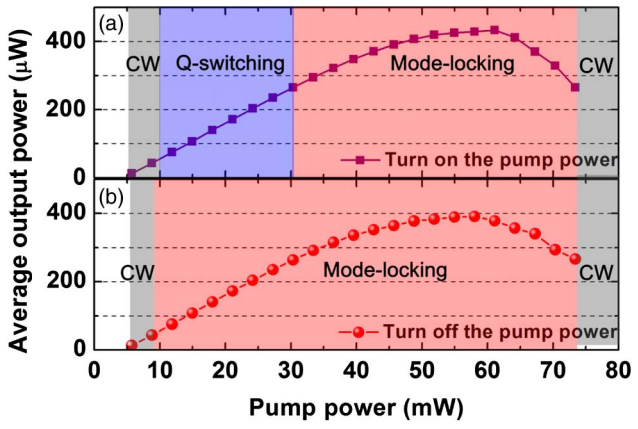

Fig. 8. Average output power as a function of the pump power when (a) turning on and (b) turning off the pump power.

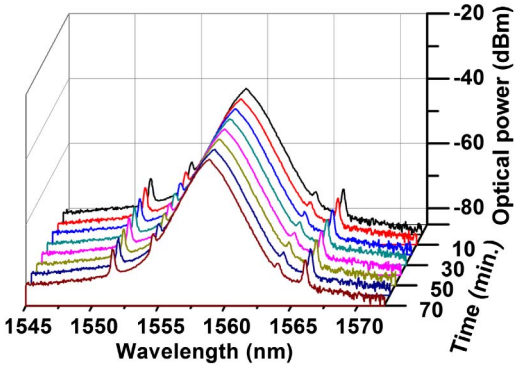

Fig. 9. Stability measurement of soliton mode locking by repeatedly scanning the output optical spectra at 10-min intervals.

In order to evaluate the long-term stability of the passive mode locking, we recorded the mode-locked optical spectrum in 10-min intervals for 70 min at the fixed pump power of 33.4 mW. Figure 9 gives the eight series of spectral data. Neither the central wavelength drift nor the power variation was significantly observed, further confirming that the mode-locked operation possesses good long-term stability.

5. CONCLUSION

We propose a new SA material, $MoSe_2$, for efficient mode locking of an EDFL. In our experiment, bulk $MoSe_2$ is exfoliated to a few-atomic-layer structure by the liquid phase exfoliation method. Then, the few-layer $MoSe_2$ is composited with PVA to construct PVA–$MoSe_2$ film as a fiber-compatible SA. The $MoSe_2$ SA is measured to have a modulation depth of 0.63% and a nonsaturable loss of 3.5% (i.e., the relative modulation depth of 18%). When inserting the $MoSe_2$ SA into an EDFL, stable mode locking is initiated to emit soliton pulses with duration of 1.45 ps. Moreover, the TPA of the few-layer $MoSe_2$ has also been observed, and we found that the TPA could significantly influence the mode-locking operation. The experimental results show that apart from MoS_2, few-layer $MoSe_2$, as one of the atomic-layered TMDs, can also serve as a potential SA for ultrafast photonics.

ACKNOWLEDGEMENT

This work was supported partially by the National Science Foundation of China (61475129, 61177044, 61107038, and 61275050), and also by the Project for Undergraduates' Innovation and Undertaking in Xiamen University (0630-ZX11A1).

REFERENCES

1. E. Hendry, P. J. Hale, J. Moger, A. Savchenko, and S. Mikhailov, "Coherent nonlinear optical response of graphene," Phys. Rev. Lett. **105**, 097401 (2010).
2. G.-K. Lim, Z.-L. Chen, J. Clark, R. G. Goh, W.-H. Ng, H.-W. Tan, R. H. Friend, P. K. Ho, and L.-L. Chua, "Giant broadband nonlinear optical absorption response in dispersed graphene single sheets," Nat. Photonics **5**, 554–560 (2011).
3. F. Benabid, J. C. Knight, G. Antonopoulos, and P. S. J. Russell, "Stimulated Raman scattering in hydrogen-filled hollow-core photonic crystal fiber," Science **298**, 399–402 (2002).
4. Z. Zhu, D. J. Gauthier, and R. W. Boyd, "Stored light in an optical fiber via stimulated Brillouin scattering," Science **318**, 1748–1750 (2007).

5. S. Y. Set, H. Yaguchi, Y. Tanaka, and M. Jablonski, "Laser mode locking using a saturable absorber incorporating carbon nanotubes," IEEE J. Lightwave Technol. **22**, 51–56 (2004).
6. T. Hasan, Z. Sun, F. Wang, F. Bonaccorso, P. H. Tan, A. G. Rozhin, and A. C. Ferrari, "Nanotube—polymer composites for ultrafast photonics," Adv. Mater. **21**, 3874–3899 (2009).
7. Q. Bao, H. Zhang, Y. Wang, Z. Ni, Y. Yan, Z. X. Shen, K. P. Loh, and D. Y. Tang, "Atomic-layer graphene as a saturable absorber for ultrafast pulsed lasers," Adv. Funct. Mater. **19**, 3077–3083 (2009).
8. Z. Sun, T. Hasan, F. Torrisi, D. Popa, G. Privitera, F. Wang, F. Bonaccorso, D. M. Basko, and A. C. Ferrari, "Graphene mode-locked ultrafast laser," ACS Nano **4**, 803–810 (2010).
9. C. Zhao, H. Zhang, X. Qi, Y. Chen, Z. Wang, S. Wen, and D. Tang, "Ultra-short pulse generation by a topological insulator based saturable absorber," Appl. Phys. Lett. **101**, 211106 (2012).
10. K. Wang, J. Wang, J. Fan, M. Lotya, A. O. Neill, D. Fox, Y. Feng, X. Zhang, B. Jiang, and Q. Zhao, "Ultrafast saturable absorption of two-dimensional MoS_2 nanosheets," ACS Nano **7**, 9260–9267 (2013).
11. H. Yang, X. Feng, Q. Wang, H. Huang, W. Chen, A. T. Wee, and W. Ji, "Giant two-photon absorption in bilayer graphene," Nano Lett. **11**, 2622–2627 (2011).
12. X. Li, Y. Wang, Y. Wang, W. Zhao, X. Yu, Z. Sun, X. Cheng, X. Yu, Y. Zhang, and Q. J. Wang, "Nonlinear absorption of SWNT film and its effects to the operation state of pulsed fiber laser," Opt. Express **22**, 17227–17235 (2014).
13. A. Martinez, K. Fuse, B. Xu, and S. Yamashita, "Optical deposition of graphene and carbon nanotubes in a fiber ferrule for passive mode-locked lasing," Opt. Express **18**, 23054–23061 (2010).
14. E. Kelleher, J. Travers, Z. Sun, A. Rozhin, A. Ferrari, S. Popov, and J. Taylor, "Nanosecond-pulse fiber lasers mode-locked with nanotubes," Appl. Phys. Lett. **95**, 111108 (2009).
15. D. Popa, Z. Sun, F. Torrisi, T. Hasan, F. Wang, and A. Ferrari, "Sub 200 fs pulse generation from a graphene mode-locked fiber laser," Appl. Phys. Lett. **97**, 203106 (2010).
16. H. Zhang, D. Tang, L. Zhao, Q. Bao, and K. Loh, "Large energy mode locking of an erbium-doped fiber laser with atomic layer graphene," Opt. Express **17**, 17630–17635 (2009).
17. Y. M. Chang, H. Kim, J. H. Lee, and Y.-W. Song, "Multilayered graphene efficiently formed by mechanical exfoliation for nonlinear saturable absorbers in fiber mode-locked lasers," Appl. Phys. Lett. **97**, 211102 (2010).
18. B. Fu, Y. Hua, X. Xiao, H. Zhu, Z. Sun, and C. Yang, "Broadband graphene saturable absorber for pulsed fiber lasers at 1, 1.5, and 2 μm," IEEE J. Sel. Top. Quantum Electron. **20**, 411–415 (2014).
19. F. Wang, A. Rozhin, V. Scardaci, Z. Sun, F. Hennrich, I. White, W. I. Milne, and A. C. Ferrari, "Wideband-tuneable, nanotube mode-locked, fibre laser," Nat. Nanotechnol. **3**, 738–742 (2008).
20. X. Liu, D. Han, Z. Sun, C. Zeng, H. Lu, D. Mao, Y. Cui, and F. Wang, "Versatile multi-wavelength ultrafast fiber laser mode-locked by carbon nanotubes," Sci. Rep. **3**, 2718 (2013).
21. Z. Luo, M. Zhou, J. Weng, G. Huang, H. Xu, C. Ye, and Z. Cai, "Graphene-based passively Q-switched dual-wavelength erbium-doped fiber laser," Opt. Lett. **35**, 3709–3711 (2010).
22. J. Liu, S. Wu, Q.-H. Yang, and P. Wang, "Stable nanosecond pulse generation from a graphene-based passively Q-switched Yb-doped fiber laser," Opt. Lett. **36**, 4008–4010 (2011).
23. J. L. Xu, X. L. Li, J. L. He, X. Hao, Y. Yang, Y. Wu, S. Liu, and B. Zhang, "Efficient graphene Q-switching and mode locking of 1.34 μm neodymium lasers," Opt. Lett. **37**, 2652–2654 (2012).
24. H. Yu, H. Zhang, Y. Wang, C. Zhao, B. Wang, S. Wen, H. Zhang, and J. Wang, "Topological insulator as an optical modulator for pulsed solid-state lasers," Laser Photon. Rev. **7**, L77–L83 (2013).
25. Y. Morel, A. Irimia, P. Najechalski, Y. Kervella, O. Stephan, P. L. Baldeck, and C. Andraud, "Two-photon absorption and optical power limiting of bifluorene molecule," J. Chem. Phys. **114**, 5391–5396 (2001).
26. R. Carriles, D. N. Schafer, K. E. Sheetz, J. J. Field, R. Cisek, V. Barzda, A. W. Sylvester, and J. A. Squier, "Invited review article: Imaging techniques for harmonic and multiphoton absorption fluorescence microscopy," Rev. Sci. Instrum. **80**, 081101 (2009).
27. H. Zhang, S. Virally, Q. Bao, L. K. Ping, S. Massar, N. Godbout, and P. Kockaert, "Z-scan measurement of the nonlinear refractive index of graphene," Opt. Lett. **37**, 1856–1858 (2012).
28. M. Zhang, E. Kelleher, F. Torrisi, Z. Sun, T. Hasan, D. Popa, F. Wang, A. Ferrari, S. Popov, and J. Taylor, "Tm-doped fiber laser mode-locked by graphene-polymer composite," Opt. Express **20**, 25077–25084 (2012).
29. A. Luo, N. Zhao, Z. Luo, H. Liu, M. Liu, X. Zheng, L. Liu, J. Liao, X. Wang, and W. Xu, "Trapping of soliton molecule in a graphene-based mode-locked ytterbium-doped fiber laser," IEEE Photon. Technol. Lett. **26**, 2450–2453 (2014).
30. D. Zen, N. Saidin, S. Damanhuri, S. Harun, H. Ahmad, M. Ismail, K. Dimyati, A. Halder, M. Paul, and S. Das, "Mode-locked thulium-bismuth codoped fiber laser using graphene saturable absorber in ring cavity," Appl. Opt. **52**, 1226–1229 (2013).
31. S. Huang, Y. Wang, P. Yan, J. Zhao, H. Li, and R. Lin, "Tunable and switchable multi-wavelength dissipative soliton generation in a graphene oxide mode-locked Yb-doped fiber laser," Opt. Express **22**, 11417–11426 (2014).
32. K. Wu, J. H. Wong, Z. Luo, C. Ouyang, P. Shum, and Z. Shen, "Phase noise and timing jitter eliminator for mode-locked lasers based on external graphene layers," in *Optical Fiber Communication Conference*, (Optical Society of America, 2011), paper OThL5.
33. Z. Luo, M. Zhou, D. Wu, C. Ye, J. Weng, J. Dong, H. Xu, Z. Cai, and L. Chen, "Graphene-induced nonlinear four-wave-mixing and its application to multiwavelength Q-switched rare-earth-doped fiber lasers," IEEE J. Lightwave Technol. **29**, 2732–2739 (2011).
34. C. Wei, X. Zhu, F. Wang, Y. Xu, K. Balakrishnan, F. Song, R. A. Norwood, and N. Peyghambarian, "Graphene Q-switched 2.78 μm Er^{3+}-doped fluoride fiber laser," Opt. Lett. **38**, 3233–3236 (2013).
35. Y.-H. Lin, C.-Y. Yang, J.-H. Liou, C.-P. Yu, and G.-R. Lin, "Using graphene nano-particle embedded in photonic crystal fiber for evanescent wave mode-locking of fiber laser," Opt. Express **21**, 16763–16776 (2013).
36. G. Sobon, J. Sotor, and K. M. Abramski, "Passive harmonic mode-locking in Er-doped fiber laser based on graphene saturable absorber with repetition rates scalable to 2.22 GHz," Appl. Phys. Lett. **100**, 161109 (2012).
37. B. Xu, A. Martinez, and S. Yamashita, "Mechanically exfoliated graphene for four-wave-mixing-based wavelength conversion," IEEE Photon. Technol. Lett. **24**, 1792–1794 (2012).
38. Z. Luo, Y. Huang, J. Weng, H. Cheng, Z. Lin, B. Xu, Z. Cai, and H. Xu, "1.06 μm Q-switched ytterbium-doped fiber laser using few-layer topological insulator Bi_2Se_3 as a saturable absorber," Opt. Express **21**, 29516–29522 (2013).
39. P. Yan, R. Lin, H. Zhang, Z. Wang, H. Chen, and S. Ruan, "Multi-pulses dynamic patterns in a topological insulator mode-locked ytterbium-doped fiber laser," Opt. Commun. **335**, 65–72 (2015).
40. P. Yan, R. Lin, S. Ruan, A. Liu, and H. Chen, "A 2.95 GHz, femtosecond passive harmonic mode-locked fiber laser based on evanescent field interaction with topological insulator film," Opt. Express **23**, 154–164 (2015).
41. Z. C. Luo, M. Liu, H. Liu, X.-W. Zheng, A.-P. Luo, C.-J. Zhao, H. Zhang, S.-C. Wen, and W.-C. Xu, "2 GHz passively harmonic mode-locked fiber laser by a microfiber-based topological insulator saturable absorber," Opt. Lett. **38**, 5212–5215 (2013).
42. H. Liu, X.-W. Zheng, M. Liu, N. Zhao, A.-P. Luo, Z.-C. Luo, W.-C. Xu, H. Zhang, C.-J. Zhao, and S.-C. Wen, "Femtosecond pulse generation from a topological insulator mode-locked fiber laser," Opt. Express **22**, 6868–6873 (2014).
43. C. Zhao, Y. Zou, Y. Chen, Z. Wang, S. Lu, H. Zhang, S. Wen, and D. Tang, "Wavelength-tunable picosecond soliton fiber laser with topological insulator: Bi_2Se_3 as a mode locker," Opt. Express **20**, 27888–27895 (2012).
44. Z. Luo, C. Liu, Y. Huang, D. Wu, J. Wu, H. Xu, Z. Cai, Z. Lin, L. Sun, and J. Weng, "Topological-insulator passively Q-switched double-clad fiber laser at 2 μm Wavelength," IEEE J. Sel. Top. Quantum Electron. **20**, 0902708 (2014).
45. J. Sotor, G. Sobon, and K. M. Abramski, "Sub-130 fs mode-locked Er-doped fiber laser based on topological insulator," Opt. Express **22**, 13244–13249 (2014).

46. Z. Dou, Y. Song, J. Tian, J. Liu, Z. Yu, and X. Fang, "Mode-locked ytterbium-doped fiber laser based on topological insulator: Bi_2Se_3," Opt. Express **22**, 24055–24061 (2014).
47. J. Lee, J. Koo, Y.-M. Jhon, and J. H. Lee, "A femtosecond pulse erbium fiber laser incorporating a saturable absorber based on bulk-structured Bi_2Te_3 topological insulator," Opt. Express **22**, 6165–6173 (2014).
48. S. Wang, H. Yu, H. Zhang, A. Wang, M. Zhao, Y. Chen, L. Mei, and J. Wang, "Broadband few-layer MoS_2 saturable absorbers," Adv. Mater. **26**, 3538–3544 (2014).
49. K. Wang, Y. Feng, C. Chang, J. Zhan, C. Wang, Q. Zhao, J. N. Coleman, L. Zhang, W. J. Blau, and J. Wang, "Broadband ultrafast nonlinear absorption and nonlinear refraction of layered molybdenum dichalcogenide semiconductors," Nanoscale **6**, 10530–10535 (2014).
50. H. Zhang, S. Lu, J. Zheng, J. Du, S. Wen, D. Tang, and K. Loh, "Molybdenum disulfide (MoS_2) as a broadband saturable absorber for ultra-fast photonics," Opt. Express **22**, 7249–7260 (2014).
51. H. Liu, A.-P. Luo, F.-Z. Wang, R. Tang, M. Liu, Z.-C. Luo, W.-C. Xu, C.-J. Zhao, and H. Zhang, "Femtosecond pulse erbium-doped fiber laser by a few-layer MoS_2 saturable absorber," Opt. Lett. **39**, 4591–4594 (2014).
52. Z. Luo, Y. Huang, M. Zhong, Y. Li, J. Wu, B. Xu, H. Xu, Z. Cai, J. Peng, and J. Weng, "1-, 1.5-, and 2-μm fiber lasers Q-switched by a broadband few-layer MoS_2 saturable absorber," IEEE J. Lightwave Technol. **32**, 4077–4084 (2014).
53. H. Xia, H. Li, C. Lan, C. Li, X. Zhang, S. Zhang, and Y. Liu, "Ultrafast erbium-doped fiber laser mode-locked by a CVD-grown molybdenum disulfide (MoS_2) saturable absorber," Opt. Express **22**, 17341–17348 (2014).
54. Y. Huang, Z. Luo, Y. Li, M. Zhong, B. Xu, K. Che, H. Xu, Z. Cai, J. Peng, and J. Weng, "Widely-tunable, passively Q-switched erbium-doped fiber laser with few-layer MoS_2 saturable absorber," Opt. Express **22**, 25258–25266 (2014).
55. R. Woodward, E. Kelleher, R. Howe, G. Hu, F. Torrisi, T. Hasan, S. Popov, and J. Taylor, "Tunable Q-switched fiber laser based on saturable edge-state absorption in few-layer molybdenum disulfide (MoS_2)," Opt. Express **22**, 31113–31122 (2014).
56. S. Tongay, J. Zhou, C. Ataca, K. Lo, T. S. Matthews, J. Li, J. C. Grossman, and J. Wu, "Thermally driven crossover from indirect toward direct bandgap in 2D semiconductors: $MoSe_2$ versus MoS_2," Nano Lett. **12**, 5576–5580 (2012).
57. J. N. Coleman, "Liquid-phase exfoliation of nanotubes and graphene," Adv. Funct. Mater. **19**, 3680–3695 (2009).
58. X. Wang, Y. Gong, G. Shi, W. L. Chow, K. Keyshar, G. Ye, R. Vajtai, J. Lou, Z. Liu, and E. Ringe, "Chemical vapor deposition growth of crystalline monolayer $MoSe_2$," ACS Nano **8**, 5125–5131 (2014).
59. L. Nelson, D. Jones, K. Tamura, H. Haus, and E. Ippen, "Ultrashort-pulse fiber ring lasers," Appl. Phys. B **65**, 277–294 (1997).
60. Q. Wang, J. Geng, Z. Jiang, T. Luo, and S. Jiang, "Mode-locked Tm–CHo-codoped fiber laser at 2.06 μm," IEEE Photon. Technol. Lett. **23**, 682–684 (2011).
61. Z. Luo, J. Wang, M. Zhou, H. Xu, Z. Cai, and C. Ye, "Multiwavelength mode-locked erbium-doped fiber laser based on the interaction of graphene and fiber-taper evanescent field," Laser Phys. Lett. **9**, 229 (2012).
62. M. Nakazawa, E. Yoshida, and Y. Kimura, "Low threshold, 290 fs erbium-doped fiber laser with a nonlinear amplifying loop mirror pumped by InGaAsP laser diodes," Appl. Phys. Lett. **59**, 2073–2075 (1991).
63. A. Hideur, T. Chartier, M. Brunel, M. Salhi, C. Özkul, and F. Sanchez, "Mode-lock, Q-switch and CW operation of an Yb-doped double-clad fiber ring laser," Opt. Commun. **198**, 141–146 (2001).
64. D. Tang, L. Zhao, B. Zhao, and A. Liu, "Mechanism of multisoliton formation and soliton energy quantization in passively mode-locked fiber lasers," Phys. Rev A. **72**, 043816 (2005).
65. A. Komarov, H. Leblond, and F. Sanchez, "Multistability and hysteresis phenomena in passively mode-locked fiber lasers," Phys. Rev. A **71**, 053809 (2005).
66. A. Komarov, H. Leblond, and F. Sanchez, "Theoretical analysis of the operating regime of a passively-mode-locked fiber laser through nonlinear polarization rotation," Phys. Rev A **72**, 063811 (2005).